Shrinking Core Model for Knudsen Diffusion-Limited Atomic Layer Deposition on a Nanoporous Monolith with an Ultrahigh Aspect Ratio

Hoo-Yong Lee,[†] Cheng Jin An,[†,‡] Shan Ji Piao, Dae Young Ahn, Mun-Tae Kim, and Yo-Sep Min*

Department of Chemical Engineering, Konkuk University, Seoul 143-701, Korea

Received: July 26, 2010; Revised Manuscript Received: September 20, 2010

ZnO was grown on nanoporous alumina monoliths by atomic layer deposition (ALD) from diethylzinc (DEZ) and water. The alumina monolith has a cylindrical shape with a length of 6.2 ± 2.0 mm and a diameter of 1.93 ± 0.78 mm, of which the average pore diameter and specific surface area are 8.9 nm and 256 m^2/g, respectively. The ALD process in the nanoporous monolith, of which the aspect ratio is higher than 10^5, was limited by the Knudsen diffusion of DEZ within the pores. The minimum exposure time (τ_{cy}) of DEZ for the complete coverage of ZnO on the cylindrical monolith was predicted to be $\tau_{cy} = \rho_{OH}R^2/4D_eC_o$ by using the shrinking core model (SCM) where ρ_{OH} is a molar volumetric density of OH groups, R is a radius of the monolithic cylinder, D_e is an effective diffusion coefficient of DEZ in porous alumina, and C_o is a concentration of DEZ on the exterior surface. Using a value of D_e (1.4×10^{-2} cm^2/s) obtained from the SCM, the minimum exposure time was predicted to be ~66 min. Indeed, the complete coverage of ZnO was experimentally accomplished in an exposure time of 70 min. In addition, it is also demonstrated that the minimum exposure time is largely dependent in the shape (e.g., planar, cylindrical, or spherical) of the monolith.

1. Introduction

Since atomic layer deposition (ALD) was introduced with the name atomic layer epitaxy in the late 1970s,[1] ALD has been mainly utilized to deposit various thin films such as dielectric, metallic, and luminescent materials for electronic applications.[2−6] Especially as the feature size of electronic devices has shrunk continuously, dielectric and metallic thin films grown by ALD have been intensively studied for transistors and capacitors.[7−9] Recently, the application field of ALD has been widened to the preparation of nanostructured materials and catalysts by using characteristic conformal growth behavior.[10−13]

ALD is a special modification of chemical vapor deposition for so-called self-limiting film growth.[2−6] In ALD, an appropriate precursor vapor and a reaction gas are alternately pulsed onto a substrate of which the temperature is maintained to be low enough to avoid thermal decomposition of the precursor. The reaction chamber is purged with an inert gas between the pulses of the precursor vapor and the reaction gas. Each cycle of ALD process generally consists of precursor pulse−purge−reaction gas pulse−purge. Consequently, film deposition occurs through chemical adsorption (i.e., chemisorption) between the gaseous molecules (i.e., precursor vapor or reactant gas) and the reactive functional groups on the surface (e.g., hydroxyl groups or chemisorbed organometallic groups). Once vacant adsorption sites become saturated by adsorbate molecules to form one monolayer (practically, the submonolayer is formed due to the bulkiness of adsorbate molecules), the precursor or reactant gas in excess does not chemically adsorb on the monolayer. Therefore, if sufficient amounts of precursor vapor and reactant gases are supplied to the substrate and byproducts and excess amounts of molecules are removed by the purging step, conformal films can be obtained on the substrate. The conformality of ALD films is because of the self-limiting growth mechanism where growth per cycle is limited by the number of vacant adsorption sites and not by the number of gaseous molecules supplied because the amount of the former is much smaller than that of the latter.

However, for a porous material with an ultrahigh aspect ratio (>10^3), the conformal coating may not be guaranteed in a typical ALD condition. It is generally accepted that ALD on porous materials with ultrahigh aspect ratios is limited mainly by Knudsen diffusion of precursor molecules.[14−22] In smaller pores, it is more difficult for the precursor to reach vacant sites in a typical exposure time of several seconds as the pore lengths are longer, even though the precursor has a high vapor pressure. Several groups suggested theoretical models for the conformality and step coverage in ALD to predict a suitable exposure time of precursor.[14,15,23] Gordon et al. predicted the exposure, which is a product of exposure time and precursor vapor pressure, needed for straight holes with a range of aspect ratios from 1 to 2000.[14] George et al. predicted minimum exposure times to achieve conformal ZnO ALD in an anodic alumina membrane by using Monte Carlo simulation.[15] Recently, Kang et al. also extended the step-coverage model in ALD to the deposition of TiO_2 films on straight holes, focusing on the effect of a precursor partial vapor pressure and a deposition temperature, as well as the number of cycles.[23]

In the practical applications of porous materials (e.g., catalysis), the pores are generally tortuous, and the porous materials have a specific shape such as sphere, cylinder, and tablet. Here, we propose a shrinking core model (SCM), which can be applicable to cylindrical, spherical, and planar monoliths with tortuous pores.[24] The minimum exposure time of precursor for the ideal conformality is predicted by using SCM. The prediction by SCM is compared with the experimental data obtained from ZnO ALD on a porous alumina monolith with a

* To whom correspondence should be addressed. E-mail: ysmin@konkuk.ac.kr.

[†] H.-Y.L. and C.J.A. contributed equally to this work.

[‡] Current address: Department of Chemical & Biomolecular Engineering, Korea Advanced Institute of Science and Technology, Daejeon 305-701, Korea.

10.1021/jp106945n
Published on Web 10/07/2010

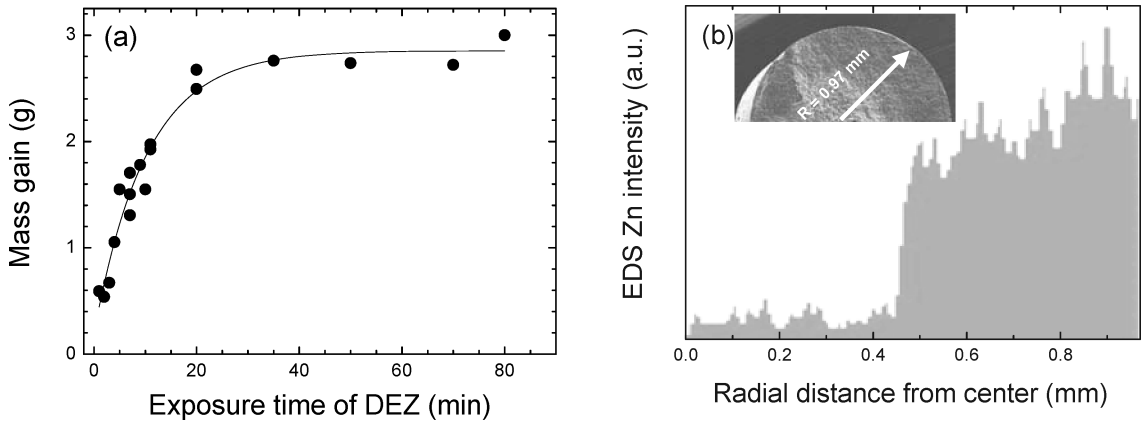

Figure 1. (a) Mass gain by one ALD cycle on 10 g of alumina as a function of exposure time of DEZ. The solid line is a guide to the eye. (b) EDS Zn profile in the circular cross-section of a 20 min-exposed monolith as a function of the radial distance from the center. The inset shows a SEM cross-sectional image of the cylindrical monolith.

cylindrical shape. The ZnO ALD was performed with diethylzinc (DEZ) and water vapor. The cylindrical monoliths have an average diameter of 1.93 mm and an average pore diameter of 8.9 nm. Therefore, the typical aspect ratio of our nanoporous monolith is $\sim 2.2 \times 10^5$.

2. Experimental Section

As a metal precursor, a reactant gas, and a porous material, we chose DEZ (electronic grade, Mecharonics), water, and alumina (cylindrical extrudate, Sasol), respectively, because two half-reactions of DEZ and water to obtain ZnO are well understood as given by[15]

$$||\text{–OH} + \text{Zn}(\text{CH}_2\text{CH}_3)_2 \rightarrow ||\text{–OZn}(\text{CH}_2\text{CH}_3) + \text{C}_2\text{H}_6 \quad (1)$$

$$||\text{–Zn}(\text{CH}_2\text{CH}_3) + \text{H}_2\text{O} \rightarrow ||\text{–ZnOH} + \text{C}_2\text{H}_6 \quad (2)$$

where the symbol ||– designates the surface species. Furthermore, DEZ is highly volatile (vapor pressure ~9.2 Torr at 15 °C) and reactive to the hydroxyl groups on the surface.[25]

The length and diameter of the cylindrical alumina monoliths are measured to be 6.2 ± 2.0 and 1.93 ± 0.08 mm, respectively, from 100 monoliths. The density of them was evaluated to be ~ 0.703 g/cm^3 from the mass and dimensions of 100 monoliths. The surface area (256 m^2/g), average pore diameter (8.9 nm), and pore volume (0.863 cm^3/g) of the monolithic cylinders are determined by Brunauer–Emmett–Teller and Barrett–Joyner–Halenda methods using an ASAP2020 Surface Area Analyzer (Micromeritics).[26] The porosity was calculated to be 0.61 from the pore volume and the density of the porous alumina monoliths.

ZnO ALD was performed on the nanoporous 10 g of alumina ($\sim 790 \pm 50$ monoliths) at room temperature. When the 10 g of alumina was loaded in an ALD reactor, the height of the loaded monolith layer was 5.5 ± 0.2 mm. DEZ and water were flowed from the bottom to the top of the loaded layer. DEZ was supplied at a flow rate of 0.29 g/min (3.7 mmol/min) without any carrier gas, and water was carried at a flow rate of 0.10 g/min (5.6 mmol/min) by N_2 gas for 1.5 h. For the purging steps, DEZ, water, and byproducts were only evacuated without any purging gas for 3.5 h. Therefore, our ALD sequence can be summarized as follows: DEZ exposure, variable times; purge, 3.5 h; water exposure, 1.5 h; and purge, 1.5 h. The base pressure of our ALD system was $\sim 6 \times 10^{-2}$ Torr, and the working pressures were 1.7–3.0 Torr for DEZ and 2.8–4.0 Torr for water.

The ZnO growth behavior was investigated with the mass gain on 10 g alumina after the ALD process. Because the total surface area of the 10 g alumina is around 2500 m^2, the mass gain due to ZnO growth is large enough to measure with a digital balance. The penetration depth of ZnO from the exterior surface into the center in the circular cross-section of the cylinder was determined from an energy-dispersive spectrometric (EDS) profile of zinc in a field emission scanning electron microscope (FE-SEM).

3. Results and Discussion

Figure 1a shows the mass gain on 10 g of cylindrical monoliths as a function of DEZ exposure time. In a typical ALD on a flat substrate, the plot of the growth thickness against the exposure time of precursor is generally used to determine the exposure time for the self-limiting growth. In our ALD on the porous monolith, the mass gain by ALD was monitored instead of the growth thickness. However, it should be noted that there are experimental errors, as shown in the scattered data points of Figure 1a, on the measurement of the mass gain, mainly due to the adsorption of ambient gases (possibly moisture) on the large surface area of the porous monolith during weighing.

All specimens for Figure 1a were prepared by one ALD cycle. The exposure of water may be enough, because water is more volatile than DEZ, and the exposure time (90 min) of water is much longer than that of DEZ. As the exposure time of DEZ increases, the mass gain due to ZnO growth rapidly increases in short exposure times. However, the slope gradually goes down in long exposure times. It seems to be the saturation of the mass gain originated from the typical self-limiting growth in ALD. If this were true, for example, the ZnO in the monolithic cylinder exposed for 20 min should be uniformly found in the circular cross-section. However, as shown in Figure 1b, the penetration depth of the ZnO from the exterior surface of the cylindrical monolith is only half the radius of the cylinder when the exposure time of DEZ is 20 min. There may be two possible cases for the incomplete coverage of DEZ on the monolith, if we assume that the two half-reactions (eqs 1 and 2) are very fast with 100% sticking coefficients: (1) an insufficient supply of DEZ molecules in comparison with the number of the adsorption sites (i.e., OH groups) and (2) the Knudsen diffusion-

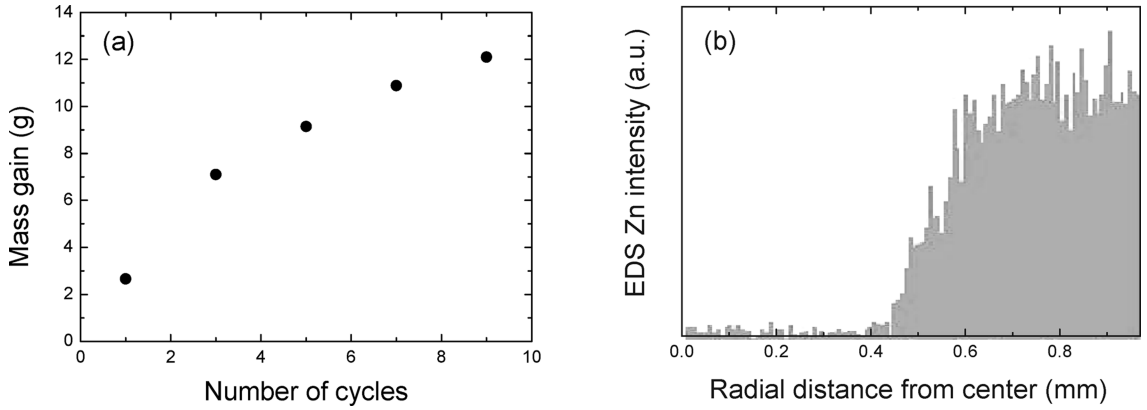

Figure 2. (a) Mass gain on 10 g of alumina as a function of the number of ALD cycles. The exposure time of DEZ is 20 min. (b) EDS Zn profile in the circular cross-section of a 10-cylced monolith as a function of the radial distance from the center.

limited ALD, which can occur when the precursor molecules move by molecular flow (i.e., no gas-phase collisions) within the pores.[14,15]

The half-reaction (eq 1) for the chemisorption of DEZ is a strong exothermic reaction, and it can be assumed that the chemisorption of DEZ, which is one of ideal precursors, has 100% sticking coefficient on the OH-terminated surface.[14,15] In general, if all of the impinging gas adsorbs on the surface, 1 Langmuir (L) represents a surface accumulation of about 1/3 monolayer in 1 cm^2.[27] Considering the total surface area of nanoporous 10 g alumina ($\sim 2.56 \times 10^7$ cm^2), the minimum exposure apparently required to form one monolayer in the whole surface is $\sim 7.7 \times 10^7$ L under the assumption of a 100% sticking coefficient. On the other hand, the exposure for the specimen on which DEZ was supplied for 20 min in a pressure range of 1.7−3.0 Torr is $2.0 \times 10^9 - 3.6 \times 10^9$ L. Therefore, the experimental exposure is large enough to exclude the insufficient supply of DEZ. Consequently, the incomplete coverage of ZnO in Figure 1b is mainly attributed to the Knudsen diffusion-limited ALD. Indeed, the mean free path (in an order of several tens of μm) of DEZ molecules in our ALD conditions is much larger than the average pore diameter (8.9 nm), which justifies the Knudsen diffusion within the pores of our cylindrical monolith.

Figure 2a shows the mass gain variation with the number of ALD cycles under the DEZ exposure time of 20 min. As the ALD sequence is repeated, the mass gain is gradually increased, but it is not linear. The nonlinear increase of the mass gain is possibly due to more severe Knudsen diffusion-limited growth of ZnO in higher numbers of cycles. This is supported by the slope of the Zn profile in Figure 2b, which was obtained from a ten-cycled monolith. While the boundary between the reacted and the unreacted regions is very sharp in the one ALD cycle specimen (Figure 1b), the boundary in Figure 2b is relatively gradual. The more severe Knudsen diffusion-limited growth in the higher ALD cycles is also supported by the curve of pore volume versus pore diameter in Figure 3. Comparing the bare (open circle) and ten-cycled (solid circle) alumina, the contribution of pores with large diameters to the pore volume is dramatically decreased in the ten-cycled monoliths, which results in more difficulty in the Knudsen diffusion.

The minimum exposure time of DEZ for the complete coverage can be predicted by using the SCM, which had been first developed by Yagi and Kunii.[24,28,29] Figure 4 represents a reacting cylindrical monolith during the DEZ exposure. R and ξ are the radii of the cylinder and the unreacted core, respectively, and C_o is the DEZ concentration in the exterior surface. In our discussion, we will focus on the first half-cycle (eq 1) for the chemisorption of DEZ. Because water has a much higher vapor pressure than DEZ and its exposure time is long enough (this will be verified at the end of this section), the penetration depth of ZnO may be decided by the Knudsen diffusion of DEZ accompanying its chemisorption. To apply the SCM to the Knudsen diffusion-limited ALD on our cylindrical monoliths, we assume the following: (1) DEZ rapidly adsorbs on OH groups of the alumina surface to form a chemisorbed monolayer without any desorption. (2) The transport of DEZ from the precursor canister to the exterior surface of the monoliths is much faster than the Knudsen diffusion within the pores. (3) The diffusion is only radial in our cylindrical monolith; thus, we ignore the diffusion along the longitudinal axis. (4) The concentration (C_o) of DEZ on the exterior surface is constant during the DEZ exposure. Under

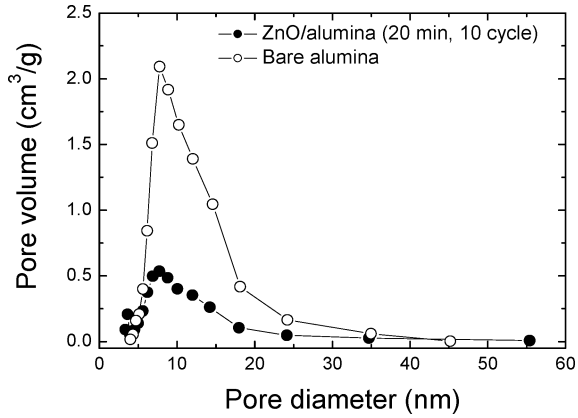

Figure 3. Pore volume of bare (open circle) and 10-cycled (solid circle) monoliths as a function of pore diameter.

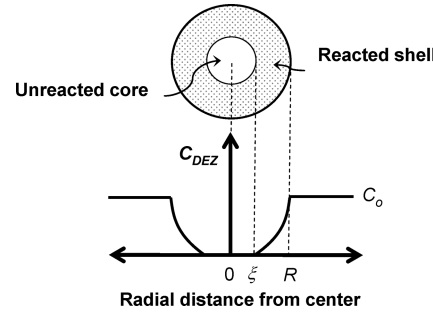

Figure 4. Representation of a reacting cylindrical monolith during the DEZ exposure. R and ξ are the radii of the cylinder and the unreacted core, respectively, and C_o is the DEZ concentration in the exterior surface.

the first assumption, the boundary between the reacted shell and the unreacted core is sharp and moves to the center in the circular cross-section as the exposure time of DEZ increases during the first half-cycle.

Using the steady-state assumption, the rate of consumption of DEZ by adsorption in the radial distance r at a time t can be approximately equal to its rate of Knudsen diffusion to the reaction surface as given by

$$-\frac{dN_{DEZ}}{dt} = Q_{DEZ} \cdot 2\pi r \cdot l \tag{3}$$

where N_{DEZ}, Q_{DEZ}, and l are the number of moles of DEZ molecules, the flux of DEZ, and the length of the monolithic cylinder, respectively. The Q_{DEZ} can be expressed by Fick's first law as below

$$Q_{DEZ} = D_e \frac{dC_{DEZ}}{dr} \tag{4}$$

where D_e is an effective diffusion coefficient of DEZ in the nanoporous monolith and C_{DEZ} is a molar concentration of gaseous DEZ within the pores. Note that both Q_{DEZ} and dC_{DEZ}/dr are positive in our coordinate system given in Figure 4. Combining eqs 3 and 4, we obtain for any radial distance r

$$-\frac{dN_{DEZ}}{dt} = 2\pi r l D_e \frac{dC_{DEZ}}{dr} \tag{5}$$

Integrating eq 5 from the exterior surface R to the boundary ξ, we obtain eqs 6 and 7 as below

$$-\frac{dN_{DEZ}}{dt} \int_R^\xi \frac{dr}{r} = 2\pi l D_e \int_{C_o}^0 dC_{DEZ} \tag{6}$$

$$-\frac{dN_{DEZ}}{dt} = 2\pi l D_e C_o/(\ln R - \ln \xi) \tag{7}$$

where we assume D_e is constant along the radial distance r. However, if there is a radial variation of the average pore diameter in the monolith, the effective diffusion coefficient should be a function of the radius, that is, $D_e(r)$. Equation 7 reveals that dN_{DEZ}/dt is constant for a given size of the unreacted core; however, as the core shrinks, the reacted shell becomes thicker, lowering the rate of the Knudsen diffusion of DEZ.

According to the first half-reaction (eq 1) for DEZ adsorption, the infinitesimal decrease of dN_{DEZ} results in the same amount of decrease in dN_{OH} (i.e., $-dN_{DEZ} = -dN_{OH}$ where N_{OH} is the number of moles of hydroxyl groups). Because N_{OH} can be rewritten with the molar volumetric density of OH groups (ρ_{OH}) and the volume of the unreacted core as below

$$-dN_{DEZ} = -dN_{OH} = -\rho_{OH}\, d(\pi \xi^2 l) = -2\pi l \rho_{OH}\, d\xi \tag{8}$$

Substituting eq 8 to eq 7 and separating variables, we obtain

$$(\ln \xi - \ln R)\, d\xi = \frac{D_e C_o}{\rho_{OH}}\, dt \tag{9}$$

Integrating eq 9 from R to ξ, we obtain

$$\int_R^\xi (\ln \xi - \ln R)\, d\xi = \frac{D_e C_o}{\rho_{OH}} \int_0^t dt \tag{10}$$

and

$$t = \frac{\rho_{OH} R^2}{4 D_e C_o}\left[1 - \left(\frac{\xi}{R}\right)^2 + \left(\frac{\xi}{R}\right)^2 \ln\left(\frac{\xi}{R}\right)^2\right] \tag{11}$$

Equation 11 can be more simplified with the minimum exposure time τ_{cy} for the complete coverage ($\xi = 0$),

$$\tau_{cy} = \frac{\rho_{OH} R^2}{4 D_e C_o} \tag{12}$$

and

$$t = \tau_{cy}\left[1 - \left(\frac{\xi}{R}\right)^2 + \left(\frac{\xi}{R}\right)^2 \ln\left(\frac{\xi}{R}\right)^2\right] \tag{13}$$

Under the assumption of the radial inward diffusion, which is considerably reasonable due to the large length-to-radius ratio (~6) in our cylindrical monolith, the surface coverage (θ) in cylindrical monolith (see the dotted line in Figure 6) can be simply expressed with

$$\theta = \frac{\pi R^2 l - \pi \xi^2 l}{\pi R^2 l} = 1 - \frac{\xi^2}{R^2} \tag{14}$$

Combining eqs 13 and 14, θ in cylindrical monolith can be related with t,

$$t = \tau[\theta + (1 - \theta)\ln(1 - \theta)] \tag{15}$$

Following similar derivation procedures for planar and spherical monoliths, respectively, the relations between t and ξ may given by

$$t = \tau_{pl}\left(1 - \frac{\delta}{L}\right)^2 \tag{16}$$

$$t = \tau_{sp}\left[1 - 3\left(\frac{\xi}{R}\right)^2 + 2\left(\frac{\xi}{R}\right)^3\right] \tag{17}$$

where L and δ are the half thicknesses of the plane and the unreacted slab for the planar monolith and τ_{pl} and τ_{sp} are the minimum exposure times of planar and spherical monoliths, respectively. These are given by

$$\tau_{pl} = \frac{\rho_{OH} L^2}{2 D_e C_o} \text{ and } \tau_{sp} = \frac{\rho_{OH} R^2}{6 D_e C_o} \tag{18}$$

Equations 12 and 18 reveal that the minimum exposure time can be shortened in smaller monoliths with lower ρ_{OH} and also reduced by using more volatile precursors with higher effective

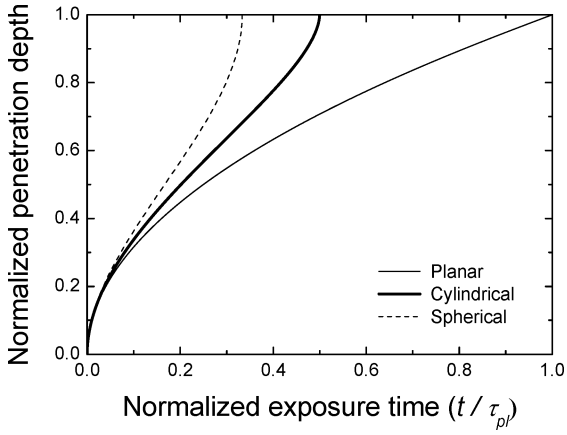

Figure 5. Normalized penetration depths of planar ($1 - \delta/L$), cylinder ($1 - \xi/R$), and spherical ($1 - \xi/R$) monoliths as a function of exposure time (t) normalized with the minimum exposure time in plane (τ_{pl}).

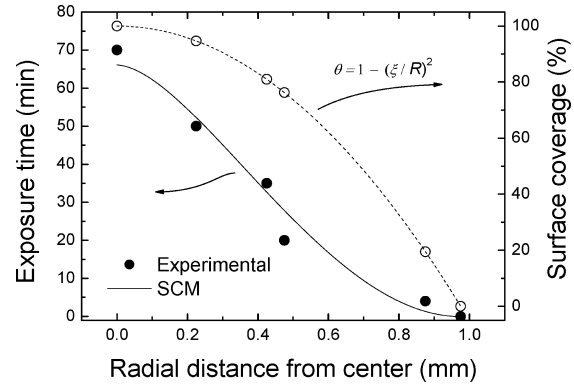

Figure 6. Experimental (solid circle) and SCM-predicting (solid line) exposure time of DEZ as a function of the radial distance from the center of the circular cross-section (left). Surface coverage calculated from eq 14. The experimental points are denoted with open circles (right).

diffusion coefficients. However, the minimum exposure times are largely dependent in the shape of monoliths. Note that τ_{pl}:τ_{cy}:τ_{sp} = 6:3:2 if all experimental conditions and materials are identical except for the shape of the monolith.

Figure 5 shows the normalized penetration depth as a function of the normalized exposure time (t/τ_{pl}). The normalized penetration depth can be defined as $1 - \xi/R$ for the cylindrical and spherical monoliths and $1 - \delta/L$ for the plane. As expected from eq 16, the normalized penetration depth in plane (thin line in Figure 5) shows the exposure time dependence of $t^{1/2}$. Elam et al. reported that the normalized ZnO coverage on anodic alumina membranes by ALD obeyed a $t^{1/2}$ time dependence.[15] Because the normalized coverage in a planar monolith can be also expressed with $1 - \delta/L$, the same time dependences of them are self-evident. However, the normalized penetration depth in cylinder or sphere does not obey the $t^{1/2}$ time dependence. Even though in a short exposure time the normalized penetration depth in cylinder (thick line) or sphere (dashed line) can be approximated with the $t^{1/2}$ time dependence, as the exposure time approaches τ_{cy} or τ_{sp}, respectively, the deviation becomes severe.

In our experimental conditions, $R = 0.097$ cm, $C_o \sim 1.1 \times 10^{-7}$ mol/cm^3 obtained from the working pressure of ~2 Torr during the DEZ exposure, and $\rho_{OH} \sim 2.6 \times 10^{-3}$ mol/cm^3 calculated by using the reported areal density (8.7 OH/nm^2) of OH groups on alumina,[30,31] specific surface area (256 m^2/g), and the density of the monolith (0.703 g/cm^3). Thus, if we know D_e of DEZ on the monolith, τ_{cy} can be predicted by eq 12.

According to the kinetic model of gases, the Knudsen diffusion coefficient (D_K) of a gas with a molecular mass M can be obtained in a porous media of a pore diameter d_p by

$$D_K = \frac{d_p}{3}\sqrt{\frac{8RT}{\pi M}} \tag{19}$$

where R is the gas constant.[32] Using the average pore diameter of 8.9 nm, D_K is around 6.7×10^{-3} cm^2/s for DEZ in our alumina monolith. If we roughly approximate D_e with D_K, $\tau_{cy} \sim 138$ min from eq 12. However, in our experiment, the complete coverage was practically accomplished at $\tau_{cy} \sim 70$ min (Figure 6). Therefore, it is expected that D_e may be much larger than D_K. The large difference may originate from the wide range of pore diameters (Figure 3), tortuosity of the pores, and other structural factors such as constriction factor, which contributes to D_e.[33] Thus, it is necessary to carefully determine D_e for the prediction of τ_{cy}, as described below.

The solid circles in Figure 6 show the exposure times of DEZ to obtain various ξ values, which were determined from the EDS profiles of one ALD cycle specimens. The experimental points were fitted with eq 13 by the least-squares method to obtain D_e as drawn with a solid line. The fitting gives $D_e \sim 1.4 \times 10^{-2}$ cm^2/s. Because there is not any reported value of D_e for DEZ in porous alumina, it is difficult to verify the fitted value. However, according to the report by Marcussen,[34] the D_e of water vapor is $\sim 3.6 \times 10^{-2}$ cm^2/s in porous alumina. Considering that the diffusion coefficient is inversely proportional to the square root of the molecular mass (eq 19), the D_e of water vapor should be 2.6 times as high as that of DEZ. Therefore, the D_e of DEZ is expected to be $\sim 1.38 \times 10^{-2}$ cm^2/s, which is close agreement with the fitted value. Using the fitted value of D_e for DEZ, the minimum exposure time of DEZ for the complete coverage ($\xi = 0$) is predicted to be ~66 min, which is well in agreement with the experimental value of 70 min.

So far, we have focused only on the first half-reaction of DEZ for the ZnO ALD. In the second half-reaction for water, we suppose that the molar volumetric density of vacant sites (i.e., ||−Zn−Et) is equal to ρ_{OH}. Using D_e of water by Marcussen and $C_o \sim 1.6 \times 10^{-7}$ mol/cm^3 from the working pressure of ~3 Torr during the water exposure, the minimum exposure time of water is ~18 min. Therefore, the water exposure time of 1.5 h in our experiments is long enough to justify the exclusion of the second half-reaction in our discussion.

4. Conclusions

ALD of ZnO was demonstrated on nanoporous alumina monoliths with a cylindrical shape of which the aspect ratio is higher than 10^5. The ALD process in the nanoporous monolith was limited by the Knudsen diffusion of DEZ within the pores. The SCM was applied to predict the minimum exposure time ($\tau_{cy} = \rho_{OH}R^2/4D_eC_o$) of DEZ for the complete coverage of ZnO on the cylindrical monolith. By fitting the experimental data with SCM, the effective diffusion coefficient of DEZ was evaluated to be $\sim 1.4 \times 10^{-2}$ cm^2/s in porous alumina. In addition, it is also demonstrated that the minimum exposure time is largely dependent on the shape of the monolith.

Acknowledgment. This work was supported by the National Research Foundation of Korea funded by the Ministry of

Education, Science and Technology (2010-0016631 and 2009-0081967). Additional funding was provided by S-Oil and SFC.

References and Notes

(1) Suntola, T., Antson, J. U.S. Patent 4,058,430, 1977.
(2) Suntola, T. *Thin Solid Films* **1992**, *216*, 84.
(3) Suntola, T. In *Handbook of Crystal Growth*; Hurle, D. T. J., Ed.; Elsevier: Amsterdam, 1994; Vol. 3, Chapter 14.
(4) Ritala, M.; Leskela, M. *Nanotechnology* **1999**, *10*, 19.
(5) Ritala, M.; Leskela, M. In *Handbook of Thin Film Materials*; Nalwa, H. S., Ed.; Academic Press: San Diego, 2002; Vol. 1, Chapter 2.
(6) Leskela, M.; Ritala, M. *Angew. Chem., Int. Ed.* **2003**, *42*, 5548.
(7) Agnello, P. D. *IBM J. Res. Dev.* **2002**, *46*, 317.
(8) Kim, H. *J. Vac. Sci. Technol., B* **2003**, *21*, 2231.
(9) Min, Y. S.; Cho, Y. J.; Hwang, C. S. *Chem. Mater.* **2005**, *17*, 626.
(10) Min, Y. S.; Bae, E. J.; Jeong, K. S.; Cho, Y. J.; Lee, J. H.; Choi, W. B. *Adv. Mater.* **2003**, *15*, 1019.
(11) Min, Y. S.; Bae, E. J.; Song, J.; Park, J. B.; Park, N. J.; Park, W.; Hwang, C. S. *Appl. Phys. Lett.* **2007**, *90*, 263104.
(12) Lindblad, M.; Lindfors, L. P.; Suntola, T. *Catal. Lett.* **1994**, *27*, 323.
(13) Rautiainen, A.; Lindblad, M.; Backman, L. B.; Puurunen, R. L. *Phys. Chem. Chem. Phys.* **2002**, *4*, 2466.
(14) Gordon, R. G.; Hausmann, D.; Kim, E.; Shepard, J. *Chem. Vap. Deposition* **2003**, *9*, 73.
(15) Elam, J. W.; Routkevitch, D.; Mardilovich, P. P.; George, S. M. *Chem. Mater.* **2003**, *15*, 3507.
(16) Kucheyev, S. O.; Biener, J.; Wang, Y. M.; Baumann, T. F.; Wu, K. J.; van Buuren, T.; Hamza, A. V.; Satcher, J. H., Jr.; Elam, J. W.; Pellin, M. J. *Appl. Phys. Lett.* **2005**, *86*, 083108.
(17) Baumann, T. F.; Biener, J.; Wang, Y. M.; Kucheyev, S. O.; Nelson, E. J.; Satcher, J. H., Jr.; Elam, J. W.; Pellin, M. J.; Hamza, A. V. *Chem. Mater.* **2006**, *18*, 6106.
(18) Elam, J. W.; Libera, J. A.; Pellin, M. J.; Zinovev, A. V.; Greene, J. P.; Nolen, J. A. *Appl. Phys. Lett.* **2006**, *89*, 053124.
(19) Elam, J. W.; Libera, J. A.; Pellin, M. J.; Stair, P. C. *Appl. Phys. Lett.* **2007**, *91*, 243105.
(20) Biener, J.; Theodore, F. B.; Wang, Y.; Nelson, E. J.; Kucheyev, S. O.; Hamza, A.; Kemell, M.; Ritala, M.; Leskela, M. *Nanotechnology* **2007**, *18*, 055303.
(21) Libera, J. A.; Elam, J. W.; Pellin, M. J. *Thin Solid Films* **2008**, *516*, 6158.
(22) Kucheyev, S. O.; Biener, J.; Baumann, T. F.; Wang, Y. M.; Hamza, A. V.; Li, Z.; Lee, D. K.; Gordon, R. G. *Langmuir* **2008**, *24*, 943.
(23) Kim, J. Y.; Kim, J. H.; Ahn, J. H.; Park, P. K.; Kang, S. W. *J. Electrochem. Soc.* **2007**, *154*, H1008.
(24) Levenspiel, O. *Chemical Reaction Engineering*, 3rd ed.; Wiley: New York, 1999; p 566.
(25) Fulem, M.; Ruzicka, K.; Ruzicka, V.; Hulicius, E.; Simecek, T.; Melichar, K.; Pangrac, J.; Rushworth, S. A.; Smith, L. M. *J. Cryst. Growth* **2003**, *248*, 99.
(26) Hrubesh, L. W.; Tillotson, T. M.; Poco, J. F. In *Chemical Processing of Advanced Materials*; Hench, L. L., West, J. K., Eds.; Wiley; New York, 1992; p 19.
(27) Smith, D. L. *Thin Film Deposition: Principles & Practice*; McGraw-Hill: New York, 1997; p 23.
(28) Yagi, S.; Kunii, D. *Chem. Eng.* **1955**, *19*, 500.
(29) Yagi., S.; Kunii, D. *Chem. Eng. Sci.* **1961**, *16*, 364.
(30) Kummert, R. Ph.D. Thesis; Swiss Fedral Institute of Technology: Zurich, 1979.
(31) Puurunen, R. L.; Lindblad, M.; Root, A.; Krause, A. O. I. *Phys. Chem. Chem. Phys.* **2001**, *3*, 1093.
(32) Brodkey, R. S.; Hershey, H. C. *Transport Phenomena: A Unified Approach*; McGraw-Hill: New York, 1988; p 183.
(33) Fogler, H. S. *Elements of Chemical Reaction Engineering*, 4th ed.; Pearson: New Jersey, 2006; p 815.
(34) Marcussen, L. *Chem. Eng. Sci.* **1970**, *25*, 1487.

JP106945N